A Measurement of the Wheel-Rail Contact Temperature Field

Chunyan He(✉), Zhen Yang, and Zili Li

Delft University of Technology, Delft 2628CK, The Netherlands
c.he-1@tudelft.nl

Abstract. As a critical factor in the degradation of rails and wheels, wheel-rail contact heat has been investigated with various analytical and numerical methods. However, the predicted temperature distributions and thermal loads have not been directly validated through measurements due to the challenges associated with accurate measurements. This study employs an infrared camera to measure the temperature variation at the wheel-rail contact under various slip ratio conditions in an in-house wheel-rail dynamic contact test rig. Wheel braking is replicated, and a wheel flat is generated. The temperature field of the contact interface is measured and analyzed, revealing the heating and cooling processes before and after the formation of the wheel flat. The results demonstrate that the contact temperature between the wheel and rail progressively increases with increasing slip ratio until a flat is formed. Notably, at a slip ratio of 8.3%, the observed contact temperature reaches 337.2 °C and then rises to 432.8 °C at a higher slip ratio of 15.9%. When the wheel flat is generated at a slip ratio of 20.4%, the observed contact temperature between the wheel and rail reaches 652.4 °C. After the formation of the flat, the contact temperature initially decreases due to more wheel material of lower temperature entering into the contact and rises again with the increase of slip ratio. These measurement findings are valuable for calibrating and validating simulation models and investigating thermal damage related to wheel-rail interactions.

Keywords: Temperature field · Continuous measurement · Wheel-rail contact · Thermal imaging · V-Track test-rig

1 Introduction

Friction generates thermal energy at the contact interface, resulting in temperature elevation. This phenomenon, known as thermal loading, can have detrimental effects on wheel-rail interfaces, such as increased rolling contact fatigue and accelerated wear rates [1, 2]. These effects are particularly significant during wheel sliding and flange contact, where friction-induced temperatures can reach very high levels. Therefore, a comprehensive understanding of the temperature field and thermal loading induced by wheel-rail contact is important for studying the deterioration of wheel-rail interfaces.

W. Huang and M. Ahmadian (Eds.): IAVSD 2023, LNME, pp. 117–123, 2025.
https://doi.org/10.1007/978-3-031-66971-2_13

Various analytical and numerical methods have been proposed to investigate thermal loading and temperature distribution at the wheel-rail interface. For instance, Knothe et al. [3] analytically calculated the sliding-induced temperature field using Laplace transforms in conjunction with Green's functions. Their analysis revealed temperatures as high as 600 °C for simulated slip ratio values of 3–4%. Lewis et al. [2] developed an analytical model to estimate the rolling contact-induced temperature field from partial slip to full slip in a scaled twin-disc setup and examined the thermal effects on material properties and wear rates. Vo et al. [4] utilized a finite element (FE) rail model subjected to multiple passes of thermal loads, employing Goldak's heat source model [5] to represent the moving thermal loads. Their simulations indicated that, with a slip ratio of 8.5%, the rail surface temperature could reach up to 522 °C after one wheel pass and 723 °C after six wheel passes. Naeimi et al. [6] proposed a 3D dynamic coupled thermomechanical FE model for wheel-rail contact, incorporating directly calculated heat sources based on tangential load and micro-slip in each element. They concluded that the maximum flash temperature of the rail in the model themo-elasto-plastic with softening is 756 °C under a 26% slip ratio. Lian et al. [7] presented a 3D FE wheel-rail contact model considering the superimposed thermal-mechanical loads resulting from multiple wheel passages. The simulated maximum flash temperature is 776.05 °C after 9 wheel passages with a slip ratio of 9.43%. However, most existing models utilize nominal thermal parameters [8], such as heat dissipation, and the solutions for thermal or thermal-mechanical loads have not been directly validated through measurements due to the challenges associated with accurately measuring the temperature field induced by wheel-rail contact [7].

Temperature fields at the interface surfaces have typically been measured using thermocouples and infrared cameras [9]. Embedded and thin-film thermocouples have been employed in certain manufacturing processes and tribology studies [10]. However, the use of embedded thermocouples requires drilling the contact bodies, which can affect contact conditions and stress distribution. Thin-film thermocouples, on the other hand, allow for temperature distribution measurement at the contact patch without drilling the contact bodies [11]. Nevertheless, wheel-rail contact imposes high contact pressures and shear stresses, which can damage thin-film thermocouples and reduce measurement accuracy. In contrast, infrared cameras can obtain the contact temperature without altering the wheel-rail contact condition. Additionally, since thermocouples cannot measure continuous temperature distributions, they may fail to capture the peak temperature at the contact interface, while infrared cameras enable continuous temperature field measurements.

In this study, a high-speed infrared camera is employed to measure the temperature field on the rail surface under various slip ratio conditions, which is replicated using a custom test rig – V-Track [12]. The correlation between slip ratio and contact temperature can be explored to investigate thermal damage at the wheel-rail interface and calibrate the thermal parameters in numerical models.

2 Methodology

The experimental setup employed in this study, i.e., the V-Track test rig (Fig. 1(a)), has been validated for replicating real-life wheel-rail frictional rolling contact and investigating the associated wheel-rail damages [13]. The test rig allows precise control and

measurement of the normal load, friction force, translational velocity, angular velocity of the wheel, and longitudinal slip ratio. To continuously capture the temperature field in the vicinity of the wheel-rail contact area, a high-speed infrared thermal imaging camera (FLIR X6900sc) is mounted on a steel frame situated on the trailing side of the wheel, as illustrated in Fig. 1(b). The camera remains in consistent alignment with the wheel assembly during movement, with a constant focus on the wheel-rail contact region. This setup enables the capture of the temperature field in proximity to and behind the trailing edge of the contact area.

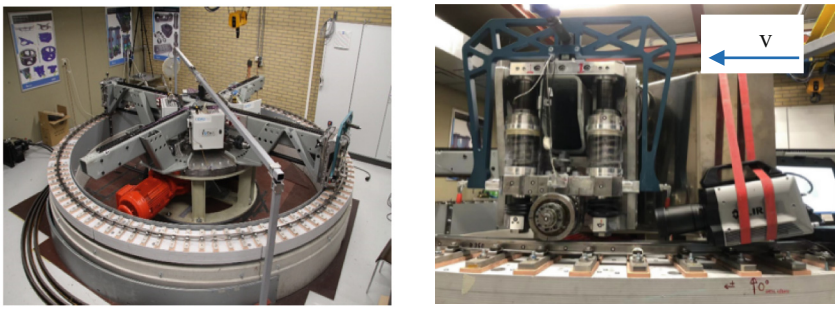

(a) An overview of the test rig

(b) The high-speed thermal camera mounted on the test rig

Fig. 1. Measurement device in V-Track.

The employed camera can acquire full 640 × 512 images at a frame rate of 1000 frames per second (1000 Hz), making it suitable for capturing rapidly changing temperature fields and flash temperatures. The camera offers different temperature ranges, namely 10–90 °C, 80–120 °C, 250–600 °C, and 500–1200 °C, which can be selected appropriately to obtain accurate temperature readings of the object. Note that real-life objects measured by the camera are not perfect black bodies; thus, they not only emit energy but also reflect ambient energy. Hence, emissivity (denoted by ε) is introduced as a term to describe the radiation efficiency of an object compared to a black body at the same wavelength, viewing angle, and temperature. The emissivity of the rail samples within different temperature ranges is measured and found to be, for example, 0.82 in the 250–600 °C range. These measured emissivity values are used to process the measured temperatures.

In this study, the measurement primarily focuses on high temperatures induced by braking since the severe wheel and rail damage can occur due to elevated thermal loads. A wheel brake is conducted using the V-Track, with the camera moving at a constant speed of 16 km/h. A braking torque, progressively increasing in magnitude, is applied until it reaches 110 N·m, at which full slip of the wheel occurs. The braking torque is then maintained until the end of the test. Over a period of 20 s (approximately 7 passages of the wheel along the track), the wheel angular speed gradually decreases from 68.5 rad/s to 3.2 rad/s, leading to a fluctuation in the wheel-rail contact temperature. The measured temperature range from 250 to 600 °C is predetermined. Once the wheel-rail contact temperature exceeds the maximum value of this range, a manual switch to a higher

range of 500 to 1200 °C is performed to continue the temperature measurement during the operation of the test rig.

3 Results

The measured thermal results are then processed and analyzed throughout the braking process. A total of 20,000 thermal images are recorded. In each thermal image, any desired section could be selected as the Region of Interest (ROI) for temperature data extraction. The ROI in this study is the area immediately behind the wheel and rail contact, encompassed by a white rectangle, as illustrated in Fig. 2. The maximum temperature within this rectangle, which varies with time, is automatically calculated. Note that the apparent temperature derived from the measurement is not the actual temperature in the contact patch due to viewing angle limitations. The observed temperature is lower than the actual temperature within the contact patch.

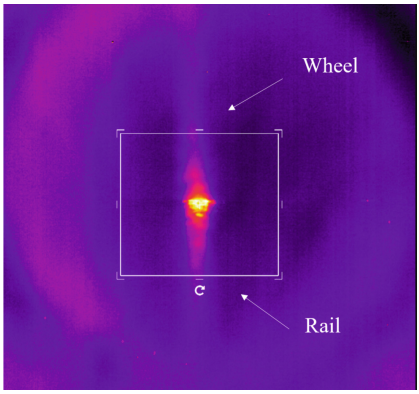

Fig. 2. Thermal image and the ROI

Figure 3 presents the variation of the maximum temperature within the ROI over time. From 0 s to 3.50 s, the observed maximum temperature of the wheel and rail remains below 250 °C. Subsequently, it gradually increases from 3.50 s to 7.97 s due to the increasing longitudinal slip ratio of the wheel and then decreases between 7.97 s and 9.60 s as more new wheel material enters into the contact area per unit time due to a surge in the slip ratio, see in the next section. At 10.90 s, the temperature reaches the maximum limit within the range of 250 to 600 °C. Then the measurement range is switched to 500 to 1200 °C, and the emissivity is adjusted accordingly. The specified emissivity can influence the values of the maximum and minimum limits of each range. For instance, the maximum limit for the range of 250 to 600 °C is 650 °C. The measurement results at four instances (t1 to t4 denoted in Fig. 3) with different temperatures are selected and analyzed subsequently.

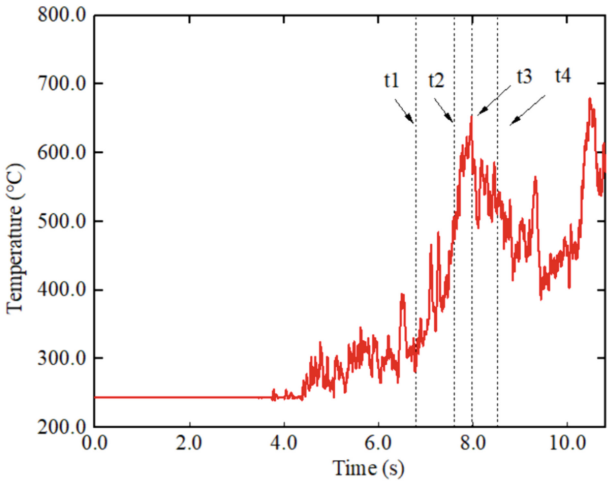

Fig. 3. The maximum temperature in the ROI varying with time

Thermal images corresponding to the four instances in Fig. 3 are displayed in Fig. 4, illustrating the wheel and rail temperature fields during the braking process. In Fig. 4(a), the observed maximum temperature within the ROI is 337.2 °C at 6.78 s. Based on the measured angular and translational velocity of the wheel, the longitudinal slip ratio at this instant is 8.3%. Figure 4(b) depicts the results at 7.61 s, where the observed maximum temperature is 432.8 °C, higher than that in Fig. 4(a) due to an increased slip ratio (15.9%). At 7.97 s, as the wheel continues braking, a wheel flat occurs as a consequence of significant material wear due to the high slip ratio and saturated friction force, as shown in Fig. 4(c). The observed maximum temperature within the ROI is 652.4 °C, and the slip ratio reaches 20.4%. Figure 4(d) showcases thermal images at the moment (8.50 s) after the wheel flat has formed. The colored area above the ROI represents the location of the wheel flat, while the patch within the ROI represents the position immediately behind the wheel and rail contact. The maximum temperature within the ROI is 529.3 °C, accompanied by a high slip ratio value of 41.4%. The involvement of more new wheel material with lower temperature "flowing" into the contact area leads to the temperature decrease.

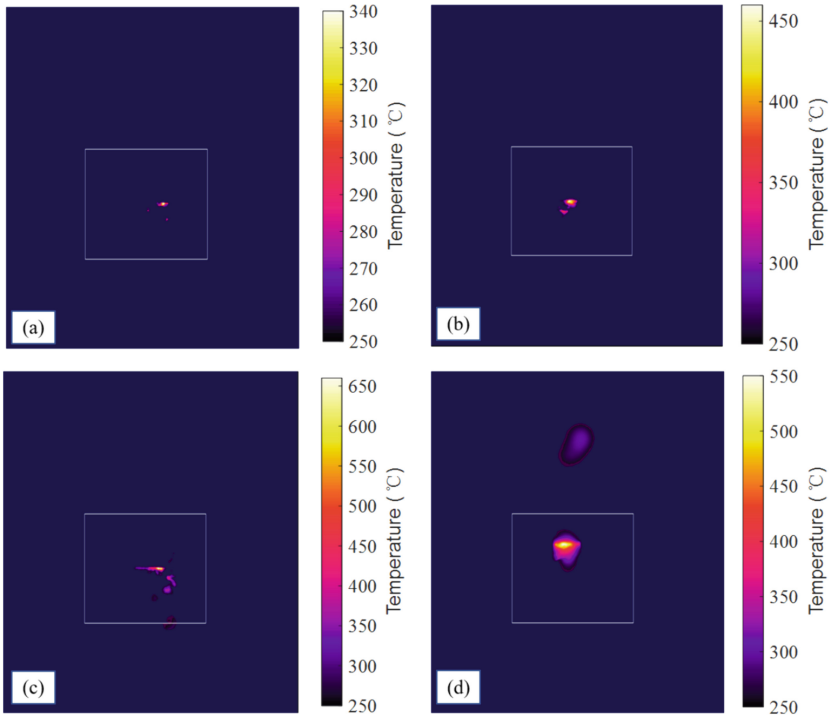

Fig. 4. Thermal images during the measurement described by the temperature at different slip ratios (denoted by s): (a) $s = 8.3\%$, (b) $s = 15.9\%$, (c) $s = 20.4\%$, (d) $s = 41.4\%$

4 Conclusions

In this study, we utilize an infrared camera to measure the temperature of the wheel-rail contact during the braking process. Temperature variation in the wheel-rail contact during braking is observed, and the formation and cooling of a wheel flat are observed. The following observations are made:

- The contact temperature between the wheel and rail progressively increases as the slip ratio increases until the formation of a wheel flat. At a slip ratio of 8.3%, the observed contact temperature between the wheel and rail reaches 337.2 °C, which further rises to 432.8 °C at a higher slip ratio of 15.9%. When the slip ratio reaches 20.4%, the observed contact temperature between the wheel and rail reaches a maximum of 652.4 °C.
- After the formation of the wheel flat, the observed contact temperature between the wheel and rail decreases. The maximum temperature within the ROI is 529.3 °C, which is lower than the temperature of 652.4 °C observed during the formation of the flat, despite the higher slip ratio value (41.4% vs. 20.4%). This temperature decrease can be attributed to the more new wheel materials of lower temperature entering into the wheel-rail interface. However, as the slip ratio continues to increase, the contact temperature gradually rises again, eventually surpassing 650 °C.

In conclusion, this study provides insights into the temperature field of the wheel-rail contact during braking, contributing to a better understanding of the thermomechanical behavior. The measured thermal results can be employed to calibrate and validate numerical simulations.

References

1. Srivastava, J.P., Sarkar, P.K., Ranjan, V.: Effects of thermal load on wheel–rail contacts: a review. J. Therm. Stress. **39**(11), 1389–1418 (2016)
2. Lewisa, R., Dwyer-Joyce, R.S.: Wear mechanisms and transitions in railway wheel steels. Proc. Inst. Mech. Eng., Part J: J. Eng. Tribol. **218**(6), 467–478 (2004)
3. Knothe, K., Liebelt, S.: Determination of temperatures for sliding contact with applications for wheel-rail systems. Wear **189**(1–2), 91–99 (1995)
4. Vo, K.D., Tieu, A.K., Zhu, H.T., et al.: The influence of high temperature due to high adhesion condition on rail damage. Wear **330**, 571–580 (2015)
5. Goldak, J., Chakravarti, A., Bibby, M.: A new finite element model for welding heat sources. Metall. Trans. B **15**, 299–305 (1984)
6. Naeimi, M., Li, S., Li, Z., et al.: Thermomechanical analysis of the wheel-rail contact using a coupled modelling procedure. Tribol. Int. **117**, 250–260 (2018)
7. Lian, Q., Deng, G., Tieu, A.K., et al.: Thermo-mechanical coupled finite element analysis of rolling contact fatigue and wear properties of a rail steel under different slip ratios. Tribol. Int. **141**, 105943 (2020)
8. Talamini, B., Gordon, J., Perlman, A.B.: Investigation of the effects of sliding on wheel tread damage. ASME Int. Mech. Eng. Congress Expos.. **42210**, 119–125 (2005)
9. Totten, G.E.: ASM handbook, Volume 18: friction, lubrication, and wear technology. ASM international, Cleveland (1992)
10. Komanduri, R., Hou, Z.B.: A review of the experimental techniques for the measurement of heat and temperatures generated in some manufacturing processes and tribology. Tribol. Int. **34**(10), 653–682 (2001)
11. Kennedy, F.E., Frusescu, D., Li, J.: Thin film thermocouple arrays for sliding surface temperature measurement. Wear **207**(1–2), 46–54 (1997)
12. Naeimi, M., Li, Z., Petrov, R.H., et al.: Development of a new downscale setup for wheel-rail contact experiments under impact loading conditions. Exp. Tech. **42**, 1–17 (2018)
13. Zhang, P., Moraal, J., Li, Z.: Design, calibration and validation of a wheel-rail contact force measurement system in V-Track. Measurement **175**, 109105 (2021)